Molecular Crystals and Liquid Crystals

Publication details, including instructions for authors and subscription information:
http://www.tandfonline.com/loi/gmcl20

# Freedericksz Transition in Nematics: Effects of Non-Linear Shear Profile and Elastic Anisotropy

Bagisa Mukherjee [a] & Arup Mukherjee [b]

[a] Penn State University, Worthington Scranton Campus, Dunmore, PA, USA

[b] Department of Mathematical Sciences, Montclair State University, Montclair, NJ, USA

Version of record first published: 05 Oct 2009

To cite this article: Bagisa Mukherjee & Arup Mukherjee (2009): Freedericksz Transition in Nematics: Effects of Non-Linear Shear Profile and Elastic Anisotropy, Molecular Crystals and Liquid Crystals, 508:1, 274/[636]-285/[647]

To link to this article: http://dx.doi.org/10.1080/15421400903065747

*Mol. Cryst. Liq. Cryst.*, Vol. 508, pp. 274/[636]–285/[647], 2009

ISSN: 1542-1406 print/1563-5287 online
DOI: 10.1080/15421400903065747



# Freedericksz Transition in Nematics: Effects of Non-Linear Shear Profile and Elastic Anisotropy

**Bagisa Mukherjee[1] and Arup Mukherjee[2]**
[1]Penn State University, Worthington Scranton Campus, Dunmore, PA, USA
[2]Department of Mathematical Sciences, Montclair State University, Montclair, NJ, USA

*Using the nematodynamic equations of Ericksen and Leslie, we investigate the nature of the Freedericksz transition for elastically anisotropic nematic liquid crystals between parallel plates and subject to a shear and an external magnetic field. Two types of velocity profiles are considered: the simplified (linear) profile where the velocity gradient in the bulk of the sample is constant and a more realistic non-linear profile. We investigate and characterize the differences in the director distortions and the onset of transition in these cases for a range of external field strengths.*

**Keywords:** elastic anisotropy; Freedericksz transition; non-linear shear profile

## 1. INTRODUCTION

Nematic liquid crystals (NLCs) exhibit long-range ordering and the direction of alignment is described by a unit vector **n** called the director. A NLC sample under the effect of an external magnetic field undergoes a Freedericksz transition beyond a critical value of the applied field. The Freedericksz transition has applications in LC devices and in experimental techniques for determining the elastic constants [1,2]. The equilibrium director alignment is determined by the interaction of the NLC with the applied field and the surface boundary effects. Derfel [3] and Blake, Mullin and Tavener [4] have studied the static Fréedericksz transition as a bifurcation problem. Recently, the authors [5] and Makarov [6] have extended the analysis

Address correspondence to Bagisa Mukherjee, Penn State University, Worthington Scranton Campus, 120 Ridge View Drive, Dunmore, PA 18512, USA. E-mail: bgm102@psu.edu

to NLCs under the influence of both a magnetic field and a shear under the simplifying assumption that the velocity gradient in the bulk of the sample is constant. In this paper, we study both flow-aligning and non-flow aligning NLCs under the influence of both a shear and an external magnetic field without this simplifying assumption.

A slight pre-tilt of approximately two degrees in the anchoring at the plates for a static NLC leads to a small variation in the critical value of the Freedericksz transition. However, this can change the measured value of the elastic constants 20%. This was experimentally observed by Rapini and Papoular [7] while Blake, Mullin, and Tavener [4] have characterized this in the language of bifurcations. Similar to this pre-tilt effect, the introduction of even very low shear can significantly affect both the critical value of the transition and the maximum director distortion. The present work deals with the characterization of the critical value of the transition and its relations to elastic anisotropy and non-linear shear profile.



## 2. DYNAMIC CONTINUUM THEORY FOR NEMATICS

For incompressible NLCs, the unit vector field $\mathbf{n}(\mathbf{x})$ represents the mean molecular alignment of a point $\mathbf{x}$ in a given sample of volume $V$ with boundary $S$. The positivity of the free energy density $\mathcal{F}$, the symmetry arising from the lack of polarity, and the fact that the molecules generally resemble rods which remain alike after reflection within planes containing $\mathbf{n}$ leads to

$$\mathcal{F}_{\mathrm{FO}}(\mathbf{n}, \nabla\mathbf{n}) = \frac{1}{2}K_1|\nabla\cdot\mathbf{n}|^2 + \frac{1}{2}K_2|\mathbf{n}\cdot(\nabla\times\mathbf{n})|^2 + \frac{1}{2}K_3|\mathbf{n}\times(\nabla\times\mathbf{n})|^2, \quad (1)$$

where the constants $K_1$, $K_2$, and $K_3$ correspond to the splay, twist, and bend elasticity (or Frank) constants. For the energy density $\mathcal{F}(\mathbf{n}, \nabla\mathbf{n})$ the total elastic energy is given by $W = \int_V \mathcal{F}(\mathbf{n}, \nabla\mathbf{n})dV$. In many NLCs, the viscoelastic response properties to applied fields can be studied using the *elastic anisotropy* $k = K_3/K_1$. External magnetic fields applied to a NLC encourages the director to align parallel to the field in the bulk of the sample. A magnetic field $\mathbf{H}$ applied to a LC sample induces a magnetization $\mathbf{M}$. If $\chi_{\|}$ and $\chi_{\perp}$ represent the magnetic susceptibilities along and perpendicular to $\mathbf{n}$ and we assume that the magnetization is linearly dependent on the applied field $\mathbf{H}$, the invariance of the elastic energy density under the transformation $\mathbf{n} \mapsto -\mathbf{n}$ leads to the expression $\mathbf{M} = \chi_{\perp}\mathbf{H} + (\chi_{\|} - \chi_{\perp})(\mathbf{H}\cdot\mathbf{n})\mathbf{n} = \chi_{\perp}\mathbf{H} + \chi_a(\mathbf{H}\cdot\mathbf{n})\mathbf{n}$, where $\mathbf{H}$ makes an arbitrary angle with $\mathbf{n}$ and the magnetic

anisotropy $\chi_a$ measures the difference between the magnetic susceptibilities and is positive for nematics. Thus, when an external magnetic field $\mathbf{H}$ is applied to a NLC, the Frank-Oseen energy of equation (1) is modified to

$$\mathcal{F} = \mathcal{F}_{\mathrm{FO}} - \int_0^H \mathbf{M} \cdot d\mathbf{H} = \mathcal{F}_{\mathrm{FO}} - \frac{1}{2}\chi_\perp H^2 - \frac{1}{2}\chi_a(\mathbf{n}\cdot\mathbf{H})^2, \text{ where } H = |\mathbf{H}|. \tag{2}$$

For this paper, we assume that the NLC is strongly anchored at the plates. Planar anchoring corresponds to the NLC sample being parallel to the boundary and homeotropic anchoring corresponds to the sample being perpendicular to the boundary.

A standard description of the motion of a fluid with microstructure involves the vector fields $\mathbf{v}(\mathbf{x}, t)$ (the velocity) and $\mathbf{w}(\mathbf{x}, t)$ (the angular velocity). For LCs, $\mathbf{w}$ represents the local angular velocity of the director $\mathbf{n}$ and thus the unit vector $\mathbf{n}$ satisfies $\dot{\mathbf{n}} = \mathbf{w} \times \mathbf{n}$, where $\dot{\mathbf{n}} = \frac{\partial \mathbf{n}}{\partial t} + \mathbf{v}\cdot\frac{\partial \mathbf{n}}{\partial \mathbf{x}}$ represents the material time derivative. If $p = p(\mathbf{x}, t)$ represents the pressure, $\rho$ the density, and $\mathbf{F}$ and $\mathbf{G}$ the external and generalized body forces, the Ericksen-Leslie nematodynamic equations for an incompressible LC sample occupying a region $V \subseteq \mathbb{R}^3$ with boundary $S$ are

$$n_i n_i = 1 \text{ and } v_{i,i} = 0, \tag{3}$$

$$\rho\dot{v}_i = \rho F_i - (p + \mathcal{F})_{,i} + \tilde{g}_j n_{j,i} + G_j n_{j,i} + \tilde{t}_{ij,j} \tag{4}$$

and

$$\left(\frac{\partial \mathcal{F}}{\partial n_{i,j}}\right)_{,j} - \frac{\partial \mathcal{F}}{\partial n_i} + \tilde{g}_i + G_i = \lambda n_i, \tag{5}$$

where $\lambda$ is a Lagrange multiplier and can be eliminated. The constitutive equations (arising from the material properties of the LC) for the viscous stress $\tilde{t}_{ij}$ and the vector $\tilde{g}_i$ are determined using the rate of strain tensor $A_{ij} = 1/2(v_{i,j} + v_{j,i})$ the vorticity tensor $W_{ij} = 1/2(v_{i,j} - v_{j,i})$ the rate of change of the director relative to the background fluid (the co-rotational time flux of the director) $N_i = \dot{n}_i - W_{ij}n_j$, and the Leslie coefficients $\alpha_i$, $1 \le i \le 6$ as

$$\tilde{t}_{ij} = \alpha_1 n_k A_{kp} n_p n_i n_j + \alpha_2 N_i n_j + \alpha_3 n_i N_j + \alpha_4 A_{ij} + \alpha_5 n_j A_{ik} n_k + \alpha_6 n_i A_{jk} n_k, \tag{6}$$

and

$$\tilde{g}_i = -\gamma_1 N_i - \gamma_2 A_{ip} N_p, \tag{7}$$

where $\gamma_1 = \alpha_3 - \alpha_2 \geq 0$ and $\gamma_2 = \alpha_3 + \alpha_2$ are the rotational viscosity and torsion coefficient and the Parodi relation $\alpha_2 + \alpha_3 = \alpha_6 - \alpha_5$ is valid. Thus, only five of the Leslie coefficients are independent and are assumed to form a canonical set of viscosities for the LC. Moreover, the Cauchy stress tensor is related to the pressure, elastic energy, and the viscous stress via $t_{ij} = -p\delta_{ij} - \frac{\partial \mathcal{F}}{\partial n_{p,j}} n_{p,i} + \tilde{t}_{ij}$. For most NLCs the rotational viscosity coefficients are of comparable magnitude and range in values from $10^{-2}$ to $10^{-1}$ poise in cgs units.

## 3. SHEAR FLOW AND FREEDERICKSZ TRANSITION

We consider time independent (steady state) solutions for a NLC trapped between two parallel plates separated by a distance $d$ and choose coordinates so that the plates are parallel to the $x$-axis and located along the lines $z = \pm d/2$ in the $xz$-plane as shown in Figure 1. We study two basic types of NLC arrangements denoted by configuration A and configuration B where the uniform external magnetic field is assumed to be $\mathbf{H} = (0, 0, H)$ and $\mathbf{H} = (H, 0, 0)$ respectively. In either case, the aligning effect of the external magnetic field and the anchoring effect at the plates act against one another. Configuration A corresponds to a magnetic field perpendicular to the NLC which has planar anchoring, while the magnetic field is parallel to the plates in configuration B and the anchoring is homeotropic. Since we consider NLCs with positive magnetic anisotropy, the director $\mathbf{n}$ tends to align in the field direction. A detailed study for both configurations was carried out in [5,6] where the authors consider the gradient of the flow velocity

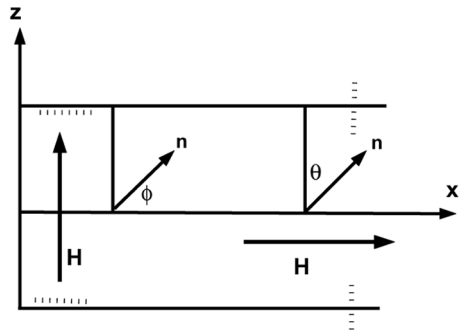


**FIGURE 1** Typical configurations. Configuration A (left portion of figure) where $H$ is perpendicular to the NLC and the anchoring (. . . . . lines) is planar and Configuration B (right portion of the figure) where $H$ is parallel to the sample and the anchoring is homeotropic.

to be linear in the bulk of the NLC. The main goal of this paper is to carefully study the difference between a linear approximation of the velocity field where $\mathbf{v} = (Uz/d,\ 0,\ 0)$ where $U$ is the velocity of the upper plate and the non-linear profile when the flow gradient is a function of $z$.

### 3.1. Configuration A

The constraints (3) are satisfied by representation if we assume $\mathbf{n} = (\cos\phi(z),\ 0,\ \sin\phi(z))$, $\mathbf{v} = (v(z),\ 0,\ 0)$, and $\mathbf{H} = (0,\ 0,\ H)$. Re-scaling the nematodynamic equations (4) and (5) by introducing a new independent variable $\tilde{z} = (z + d/2)/d$ yields

$$\frac{dv}{d\tilde{z}} = \frac{c}{g(\phi)} \tag{8}$$

and

$$f_A(\phi)\frac{d^2\phi}{d\tilde{z}^2} + \frac{1}{2}\frac{df_A(\phi)}{d\phi}\left(\frac{d\phi}{d\tilde{z}}\right)^2 = -\lambda \sin 2\phi + \mu_1 \frac{dv}{d\tilde{z}}(1 - \gamma\cos 2\phi), \tag{9}$$

where $f_A(\phi) = \cos^2\phi + k\sin^2\phi,\ \lambda = \chi_a H^2 d^2/2K_1,\ \mu_1 = \gamma_1/2K_1$, and

$$g(\phi) = \frac{1}{2}[2\alpha_1 \sin^2\phi\cos^2\phi + (\alpha_5 - \alpha_2)\sin^2\phi + (\alpha_3 + \alpha_6)\cos^2\phi + \alpha_4]. \tag{10}$$

The function $f_A(\phi) \equiv 1$ and the term involving the derivative of $f_A(\phi)$ in the second equation is absent when the NLC is elastically isotropic ($k = 1$). For isotropic fluids the function $g(\phi)$ equals the Newtonian viscosity $1/2\alpha_4$ and the velocity $v(z)$ is linear in $z$ while for a general NLC the scaled total shearing force $c$ can be determined by the shear stress required to keep the lower plate in place. The parameter $\lambda$ represents the square of dimensionless magnetic field strength and $\gamma = -\gamma_2/\gamma_1$ is the reactive parameter. When $\gamma \geq 1$ the flow alignment angle (Leslie angle) is defined as $\cos 2\phi_L = 1/\gamma$ [2]. In the absence of applied fields, the velocity gradient of a flow-aligning NLC aligns the director at the Leslie angle $\phi_L$ to the flow (it is assumed that $\phi_L$ is an acute angle).

Our analysis and computations using configuration A in Section 3 are based on the boundary value problem

$$f_A(\phi)\frac{d^2\phi}{d\tilde{z}^2} + \frac{1}{2}\frac{df_A(\phi)}{d\phi}\left(\frac{d\phi}{d\tilde{z}}\right)^2 = -\lambda \sin 2\phi + \frac{\mu}{g(\phi)}(1 - \gamma\cos 2\phi) \tag{11}$$

with boundary conditions $\phi(0)=\phi(1)=0$ (planar anchoring) where $\mu=\mu_1 c=\gamma_1 c/2K_1$. In the absence of flow and magnetic fields ($\lambda$, $\mu=0$) the boundary value problem (11) has the uniform solution $\phi\equiv 0$ corresponding to an undistorted director state. Further, for $\mu=0$ (no flow) or for $\gamma=1$, $\mu\neq 0$, and $g(\phi)=1/2\alpha_4$ (linearized flow assumption in a special NLC where the magnitudes of the rotary viscous coefficient $\gamma_1$ and the irrotational torque coefficient $\gamma_2$ are equal) the undistorted director state is a solution for arbitrary values of the magnetic field strength parameter $\lambda$. When $\gamma=1$, $\mu\neq 0$ and $g(\phi)=1/2\alpha_4$, the solution $\phi(\mathrm{z})\equiv 0$ is unstable beyond a critical value $\lambda_c=\pi^2/2$, and for $\lambda>\lambda_c$ non-uniform equilibrium states corresponding to non-constant $\phi(\mathrm{z})$ for the director exist. Positive (respectively negative) values of $\phi$ correspond to anti-clockwise (respectively clockwise) distortions of the director. This threshold value for the Freedericksz transition is identical to the threshold value for the static transition when $\gamma=1$, but the symmetry of the non-trivial solutions for $\lambda>\lambda_c$ under the transformation $\phi\mapsto-\phi$ is lost due to the influence of shear ($\mu\neq 0$). When the reactive parameter $\gamma\neq 1$, an undistorted director state exists for shear flows of arbitrary intensity ($\mu\neq 0$). The sharp phase transition of the $\gamma=1$ case is smoothed out to give a continuous branch which exists for arbitrary values of $\lambda$ and two branches which exist for values of $\lambda$ beyond a critical value $\lambda_c$. The branch point $\lambda_c$ where the sharp transition from undistorted to distorted equilibrium states occurs when $\mu=0$ or $\mu\neq 0$, $\gamma=1$, and $g(\phi)=1/2\alpha_4$ is smaller than the limit point where the bifurcation occurs for NLCs with $\gamma\neq 1$. For a detailed discussion of the combined effect of magnetic fields and a constant shear gradient on NLCs, see [5,6].

## 3.2. Configuration B

The constraints (3) are satisfied by representation if we assume $\mathbf{n}=(\sin\theta(z),\ 0,\ \cos\theta(z))$, $\mathbf{v}=(v(z),\ 0,\ 0)$, and $\mathbf{H}=(H,\ 0,\ 0)$ as show in Figure 1. Scaling and calculations similar to the previous section yield the differential equation

$$f_B(\theta)\frac{d^2\theta}{d\tilde{z}^2}+\frac{1}{2}\frac{df_B(\theta)}{d\theta}\left(\frac{d\theta}{d\tilde{z}}\right)^2=-\lambda\sin 2\theta-\frac{\mu}{g(\theta)}(1+\gamma\cos 2\theta) \qquad (12)$$

for $\theta(z)$ (the angle of the director from the vertical) satisfying the homeotropic boundary conditions $\theta(0)=\theta(1)=0$, where $f_B(\theta)=\sin^2\theta+k\cos^2\theta$ and $\lambda$, $\mu$, $\gamma$, $k$, and $g(\theta)$ have the same expressions as in Section 3.1. When both $\lambda$ and $\mu$ are non-zero, the undistorted solution

$\theta(z) \equiv 0$ solves the boundary value problem (12) only if $\gamma = -1$. However, for NLCs with rod-like molecules that we consider here, the reactive parameter $\gamma$ is positive and hence this undistorted solution is infeasible for configuration B. For $\gamma > 0$ (both non-flow aligning and flow-aligning rod-like NLCs) a continuous branch of the solution exists for all values of $\lambda$ and two branches of solutions exist beyond a limit point $\lambda_c$. The location of the branches (clockwise distortions correspond to $\theta > 0$ and anti-clockwise distortions correspond to $\theta < 0$) is determined by the value of $\gamma$. For flow-aligning NLCs ($\gamma > 1$) the continuous branch of the solution arises for $\theta > 0$ while it corresponds to negative values of $\theta$ when $0 < \gamma < 1$.

## 4. NONLINEAR FLOW PROFILE

In this section, we analyze the effect that non-linear velocity profiles have on the nature of the limits points and director distortions discussed in Sections 3.1. and 3.2. Our studies are based on two flow aligning NLCs and one non-flow aligning NLC. In order to understand the effect of non-linear flow profiles, we solve the boundary value problems (11) and (12) using both the isotropic fluid approximation (when the function $g$ is a constant $= 1/2\alpha_4$) and the true NLC expression for $g$ in equation (10). The boundary value problems are solved using the software XPPAUT [8] which can track solutions through turning points and branch points. Since the elastic anisotropy coefficient $k$ and the reactive parameter $\gamma$ are ratios of similar NLC coefficients, they are unit independent. Moreover, as shown in [5,6] typically $0 \leq \lambda \leq 15$, and $\mu \approx 1$ (in cgs units). The specific values of the NLC materials used for our study are given in Table 1. The values for

**TABLE 1** Physical Parameters for 5CB Near 32°, 5CBI (Idealized 5CB with $\alpha_1 = 0$ and $k = 1$), MBBA Near 25° and 8CB Near 37°

| Quantity | 5CB (SI) | 5CBI (SI) | MBBA (SI) | 8CB (cgs) |
|---|---|---|---|---|
| $\alpha_1$ | −0.0021 | 0 | −0.0181 | 0.38 |
| $\alpha_2$ | −0.04815 | −0.04815 | −0.1104 | −0.59 |
| $\alpha_3$ | −0.00315 | −0.00315 | −0.001104 | 0.0305 |
| $\alpha_4$ | 0.0512 | 0.0512 | 0.0826 | 0.52 |
| $\alpha_5$ | 0.03765 | 0.03765 | 0.0779 | 0.47 |
| $\alpha_6$ | −0.01365 | −0.01365 | −0.0336 | −0.084 |
| $K_1$ | $0.4 \times 10^{-11}$ | $0.4 \times 10^{-11}$ | $0.6 \times 10^{-11}$ | $12 \times 10^{-7}$ |
| $K_2$ | $0.2 \times 10^{-11}$ | $0.4 \times 10^{-11}$ | $0.38 \times 10^{-11}$ | $5.6 \times 10^{-7}$ |
| $K_3$ | $0.485 \times 10^{-11}$ | $0.4 \times 10^{-11}$ | $0.75 \times 10^{-11}$ | $12 \times 10^{-7}$ |
| $\gamma$, $k$ | 1.14, 1.2125 | 1.14, 1 | $1.\overline{02}$, 1.25 | 0.9017, 1 |

5CB and 5CBI are taken from [9–11] where the special choices for $\alpha_1$ and $k$ in 5CBI are justified, while the values for MBBA at 25° and 8CB at 37° are from [10,12,13], [2, pp. 330] and [14,15] respectively. Notice that 5CB, 5CBI, and MBBA are flow-aligning NLCs while 5CBI and 8CB are elastically isotropic. All figures in Sections 4.1. and 4.2. represent the average director distortion ($\phi(z)$ or $\theta(z)$) for $0 \leq z \leq 1$ as a function of the magnetic field strength parameter $\lambda$.

## 4.1. Flow Aligning NLCs

Figure 2 shows the differences in behavior of 5CBI when we consider $g(\phi)$ given by Eq. (10) and a constant $g(\phi)$ at a non-zero shear rate given by $\mu = 0.1$. The average director distortion is smaller for anticlockwise distortions (continuous branch on upper half) while the distortion is larger for clockwise distortions (lower branch in lower half) under the linear velocity profile assumption. Moreover, the limit point for the transition occurs at $\lambda \approx 3.97$ when we consider the linear velocity approximation while the transition occurs at a significantly higher value $\lambda \approx 5.033$ for the non-linear profile in 5CBI. Figure 3 shows the difference in behavior of 5CB and 5CBI under a shear corresponding to $\mu = 0.1$ and a non-linear velocity profile. The solid lines in Figures 3 and 2 are identical, and the dashed line in Figure 3 shows that the inclusion of elastic anisotropy and the non-zero value of $\alpha_1$ does not have a significant effect on the clockwise or anticlockwise distortions of the director. The dominant bend effect

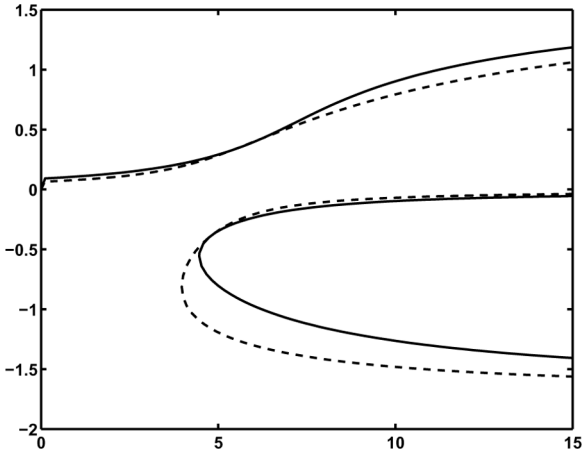


**FIGURE 2** Constant $g(\phi) = 1/2\alpha_4$ (- - - -) and non-linear velocity (——) for 5CBI configuration A.

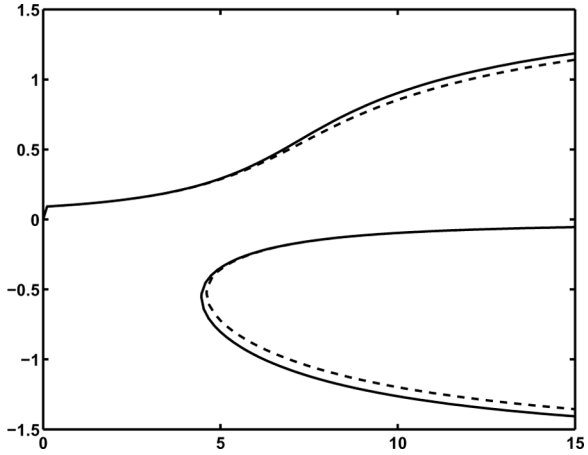


**FIGURE 3** 5CBI (——) and 5CB (- - - -) for configuration A with non-linear velocity profile.

present in 5CB ($k > 1$ or $K_3 > K_1$) results in a decrease in the distortion of the director. Changes in the value of the parameter $\mu$ (while it stays in the regime where the current assumptions about the models remain valid) do not affect the basic structure of the director distortions and their dependence on $\lambda$. Figures 4 and 5 show typical variations in the director distortions for MBBA in configuration A and B. In Figure 4, an increase in the shear constant $\mu$ causes a decrease in the

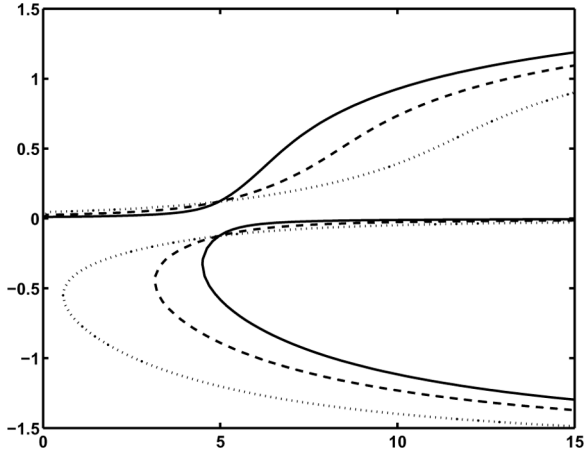


**FIGURE 4** MBBA configuration A. $\mu = 0.1$ ——, $\mu = 0.25$ - - - -, and $\mu = 0.5$ .....

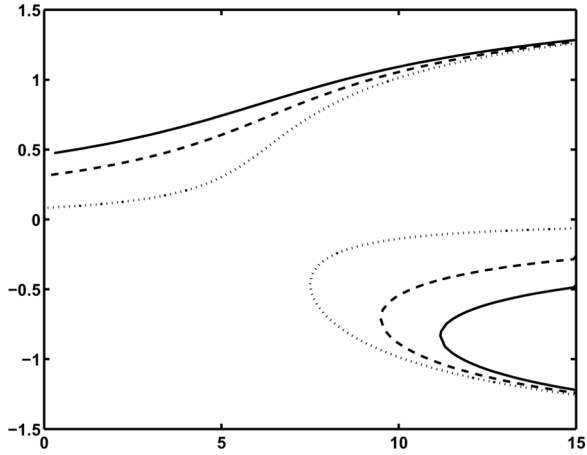


**FIGURE 5** MBBA configuration B. $\mu = 0.1$ ——, $\mu = 0.05$ - - - -, and $\mu = 0.01$ ·····.

anti-clockwise (positive branch) director distortion and an increase in the clockwise (negative branch) distortions of the director. Moreover, the numerical magnitude of the limit point (where the lower branch turns) decreases with increase in $\mu$. On the other hand, Figure 5 shows that for configuration B, the largest distortion (clockwise/positive or anticlockwise/negative) seems to be independent of the shear parameter $\mu$ for large enough values of $\lambda$. Since the shear and the magnetic

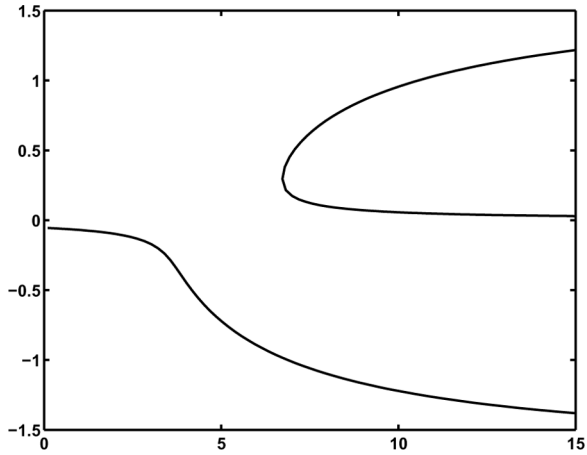


**FIGURE 6** 8CB configuration A, $\mu = 1$.

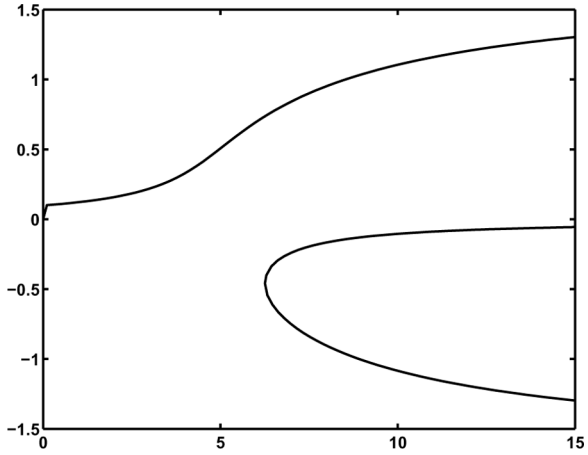


**FIGURE 7** 8CB configuration B, $\mu = 0.1$.

field work in tandem for configuration B, we expect the distortion of the director to be uniform in the bulk of the NLC for a large enough shear rate. The straightening of the upper branch of the solution in Figure 5 reiterates our intuition. As the shear rate increases, very sharp boundary layers develop at the plates.

## 4.2. Non-Flow Aligning Nematics

Figures 6 and 7 show the nature of the director distortions for the non-flow aligning NLC 8CB for configuration A and B (respectively). As seen in Figure 5 (respectively, Figure 7) for configuration B, the continuous branch of the solution which exists for all values of $\lambda$ is positive for flow aligning (respectively non-flow aligning) NLCs. However, this corresponds to anti-clockwise distortions of the director in flow-aligning NLCs and clockwise distortions of the director for non-flow aligning NLCs. On the other hand for configuration A, the continuous branch is positive for flow-aligning NLCs (Figure 4 anti-clockwise distortions) and negative for non-flow aligning (Figure 6 anti-clockwise distortions).

## 5. SUMMARY

The linear velocity approximation underestimates the anti-clockwise director distortions and over-estimates the clockwise ones for 5CBI in Configuration A (other flow-aligning nematics behave similarly).

Moreover, the linear velocity approximation predicts a significantly lower value of the limit point of the transition. For flow-aligning nematics in Configuration A, magnetic field strengths beyond a critical value results in a decrease of the maximum anti-clockwise director distortion when the shear increases while the maximum clockwise director distortion increases with increasing shear rates. On the other hand, for high enough values of the magnetic field, both the clockwise and anticlockwise distortions are independent of the shear rate in Configuration B.

## REFERENCES

[1] Chandrasekhar, S. (1992). *Liquid Crystals*, Cambridge University Press.
[2] Stewart, I. W. (2004). *The Static and Dynamic Continuum Theory of Liquid Crystals*, Taylor & Francis.
[3] Derfel, G. (1988). *Liq. Cryst.*, *3*, 1411.
[4] Blake, G. I., Mullin, T., & Tavener, S. J. (1999). *Dyn. Stab. Syst.*, *14*, 299.
[5] Mukherjee, A. & Mukherjee, B. (2005). *Phys. Rev. E*, *71*, 021703.
[6] Makarov, D. V. & Zakhlevnykh, A. N. (2006). *Phys. Rev. E*, *74*, 041710.
[7] Rapini, A. & Papoular, M. (1969). *J. D. Physique Colloq*, *30C4*, 54.
[8] Ermentrout, B. (2002). *Simulating, Analyzing, and Animating Dynamical Systems*, SIAM.
[9] Kneppe, H., Schneider, F., & Sharma, N. K. (1981). *Ber. Bunsenges. Phys. Chem.*, *85*, 784.
[10] Kneppe, H., Schneider, F., & Sharma, N. K. (1982). *J. Chem. Phys.*, *77*, 3203.
[11] Leslie, F. M., McIntosh, J. G., & Sloan, D. M. (1997). *Contin. Mech. Thermodyn.*, *9*, 293.
[12] Haller, I. (1972). *J. Chem. Phys.*, *57*, 1400.
[13] Kneppe, H., Schneider, F., & Sharma, N. K. (1981). *Mol. Cryst. Liq. Cryst.*, *65*, 23.
[14] Larson, R. G. (1993). *J. Rheol*, *37*(2), 175.
[15] Zuniga, I. & Leslie, F. M. (1989). *Liq. Cryst.*, *5*, 725.